Analysis of port breakwater boundaries in optimizing fishing areas in Batang integrated industrial area

[1]Okto R. Manullang, [2]Andi Prasetiawan, [1]Paldibo A. Sitorus

[1] Department of Urban and Regional Planning, Faculty of Engineering, Diponegoro University, Tembalang, Semarang, Central Java, Indonesia; [2] Merchant Marine Polytechnic Semarang, Semarang, Central Java, Indonesia. Corresponding author: O. R. Manullang, oktomanullang@lecturer.undip.ac.id

Abstract. The Covid-19 pandemic has caused many changes in life situations and prompted the Indonesian Government to make a strategy by developing industrial estates in the context of national economic recovery. One of the prioritized locations to become an industrial area is the Batang Integrated Industrial Estate with the support of the Container Port. Considering that the sea side of the industrial area is an area of fishing activity, it is certain that there will be lost fishing grounds due to the construction of the port. This study aims to analyze the types of boundary breakwaters in the port that are appropriate for optimizing fishing grounds. The results show that technically the offshore breakwater design does not interfere with port activities, so that 77.19% of the total area that has the potential to be lost if using shore connected breakwater can still be used for fishing activities.
Key Words: breakwaters, container ports, fishing areas, industrial estates.

Introduction. The Covid-19 pandemic has caused adversity in every part of life in the world (Wan et al 2020), including Indonesia. The slumped economy and many people lost their jobs illustrate a situation where the Government is forced to make strategies and policies that are able to save their citizens. The Government of Indonesia is seriously about developing industrial estates in the context of national economic recovery. The presence of the industrial area is required to be able to create various economic activities (Farliana et al 2020), so that the area will be used as one of the most effective tools to create jobs, boost the economy, and increase market competitiveness.

One of the prioritized locations to become an industrial area is the Batang Integrated Industrial Estate. Due to the current situation, site development has been included in the National Strategic Program which is clearly shown by the acceleration of its development so that it is hoped that it will be able to save the economy at the regional and national levels. The development of the Batang Integrated Industrial Estate is mandated by Presidential Regulation (Perpres) Number 79 of 2019 and Presidential Regulation No. 109 of 2020.

Not only industry will be built in one location, but this location will be integrated with distribution nodes consisting of trains and container ports. Dunford & Yeung (2020) conclude that one of the advantages of opening a port near an industrial area is reducing transportation costs, this is intended to increase effectiveness and efficiency in generating potential income for the country.

It should be considered that the location of the port and industrial area intersects with fishing grounds. With the existence of the port, there will be fishing areas that will be lost. In fact, the purpose of developing industrial estates that are integrated with ports is to restore the national economy. Isn't it ironic when there is an economic recovery strategy but on the other hand it eliminates fishermen's livelihoods?

There are several studies that discuss how industrial estates are brought closer to distribution nodes, both in terms of efficiency and economic impact (Ditty & Rezende

2014; Dunford & Yeung 2020; Park & Dossani 2020). However, this study aims to identify how port development still supports fishing activities. Identification is focused on optimizing fishing areas with the right type of breakwater boundaries, where both activities, fishing areas and port activities can run by minimizing the potential for conflict.

Literature review and methods

Traditional shipping and fishermen. The fisheries sector in Indonesia plays an important role in supporting national food security, because most people live in coastal areas and fish is one of the main components in the community's diet. It is estimated that six million Indonesians made a living from fishing in 2015-2016. The fishing industry in Indonesia is heavily dominated by small-scale fishermen, with 90-95% of fish production estimated to come from this sector (FAO 2014; Ariansyach 2017; Warren & Steenbergen 2021). The seaside area of the Batang Integrated Industrial Estate, namely the Java Sea, is a fishing area for small-scale fishermen. According to Purwanto (2003), The Java Sea is the main fishing area in Indonesia which accounts for 31% of the national marine fishery production. Data from the Central Statistics Agency (BPS 2020) for Batang Regency in 2015-2019 shows that the fisheries sector contributes 20% to the regional GRDP. This figure looks significant even though the Realization of Batang Regency's Original Regional Revenue (PAD) from the fisheries sector in 2020 decreased (still around Rp. 3.5 billion from the target of Rp. 4.2 billion), due to pandemic conditions and nature that was not friendly to fishermen. Bearing in mind that the construction of a supporting port for the Batang Integrated Industrial Estate is included in the National Economic Recovery strategy (Government Regulation of the Republic of Indonesia Number 23 Year 2020, issued 11 May 2020), it is necessary to see the activities of fishermen as part of social protection. It is very important to maintain this area by creating a synergy between the activities of the port to be built and the activities of existing fishermen to ensure that the economic recovery strategy has a direct impact on the community, especially fishermen in existing waters.

Breakwater in the harbor. Broadly speaking, there are two types of breakwater construction, namely shore-connected breakwater and offshore breakwater (CERC 1984). Shore-connected breakwater is a type of structure that connects directly to the beach or land, while offshore breakwater is a breakwater construction that is not connected to the shoreline and is made parallel to the coast and is at a certain distance from the shoreline. This building is designed to protect the beach that lies behind it from wave attack and can be designed in such a way that it allows wave runoff which can reduce the formation of cache, namely sediment deposits behind the structure.

Breakwaters must be designed so that ocean currents and waves do not cause siltation because the sand that is involved in the current settles in the harbor pool. If this happens then the port needs to be dredged regularly (Bonar 2014). The long-term impact resulting from the construction of a breakwater at the Supporting Port of the Batang Industrial Estate is saving on port maintenance costs in terms of dredging ponds and grooves while minimizing damage to the wharf. This needs to be done considering that the nearest existing port, namely Tanjung Emas, requires a large dredging cost, around 44.5 billion rupiah per year.

Research methods. The research was conducted from August 2020 to March 2021 at the Batang Integrated Industrial Estate, Central Java, Indonesia (see Figure 1). Observation points have been provided consisting of 2 points Acoustic Doppler Current Profiler (ADCP) for measuring 3-dimensional velocity in the water column and wave profile, 4 points Current Meter (CM) to measure the speed of water, and 1 point for tidal wave measurement (Tide). In particular, the research will discuss the sea side of the prospective supporting port for the Batang Integrated Industrial Estate which is located at Plabuan Station. The research was conducted through field observations with a case study approach. Data collection was carried out by conducting a desk study based on the results of a port technical survey conducted by Pelindo 3 in the Feasibility Study for the

Provision of Supporting Ports for the Batang Integrated Industrial Estate. The data includes surveys of Bathymetry, Ocean Hydrography, and Ocean Waves. Supporting information was also obtained by interviewing Pelindo 3, KSOP Class 1 Tanjung Emas, Batang Regency BAPPEDA, and the Batang Regency Transportation Service. The data from the port technical survey will then be analyzed to produce an Analysis of the Physical Environmental Condition of the Port Location along with Modeling when the port uses Breakwater. Then, to identify the area of fishing grounds, GIS tools will be used. The following is a distribution of data collection points related to this research.

Figure 1. Distribution of observation location points.

Results

Existing bathymetric data and analysis. The graph of the depth of each fix point depicted in the echosounder device display during the sounding work, then digitized so that the seafloor depth figures of all fix points are obtained. The depth figure that is read from the bathymetry measurements paper is the measured seabed depth from the transducer to the bottom (Figure 2). To get the mapped depth, namely the depth of the Map Datum, in this case the height of the low water spring (LWS), the calculation is carried out using the following equation:

$$Hplot = Hm + HT + Htid + Hbc$$

where: Hplot = the depth of the fix point to be plotted in the bathymetry map is the depth of the seabed from the LWS;

Hm = the depth that is read from the device display is: the depth of the seabed from the transducer;

HT = transducer depth from water level;

Htid = water level at fix point, measured from LWS;

Hbc = depth correction from Barcheck.

Bathymetry measurements is carried out in the planned area of the provision of the supporting port for KIT Batang with intervals of 75-100 meters of bathymetry.

Based on the results of interviews with Pelindo 3, the maximum dimensions of the ship planned to dock require a depth of 9 m low water spring (mlws), so the depth of the pond planned for the construction of the supporting port for the Batang Integrated Industrial Estate is 10 mlws. Figure 3 shows that the natural draft distance to reach that depth from the shoreline to that depth is ±3,600 m.

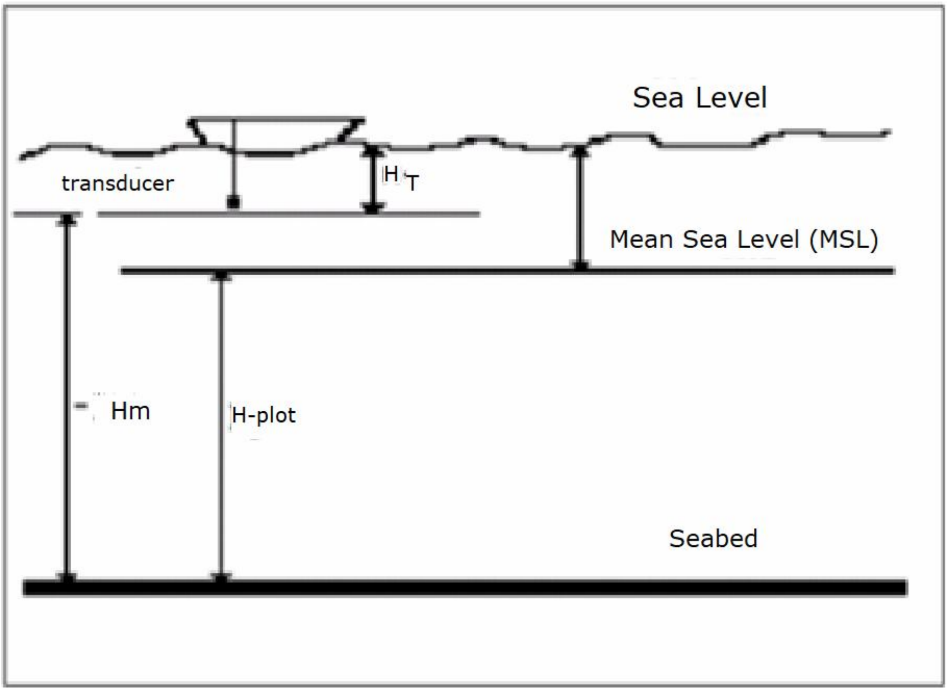

Figure 2. Ocean depth correction calculation sketch.

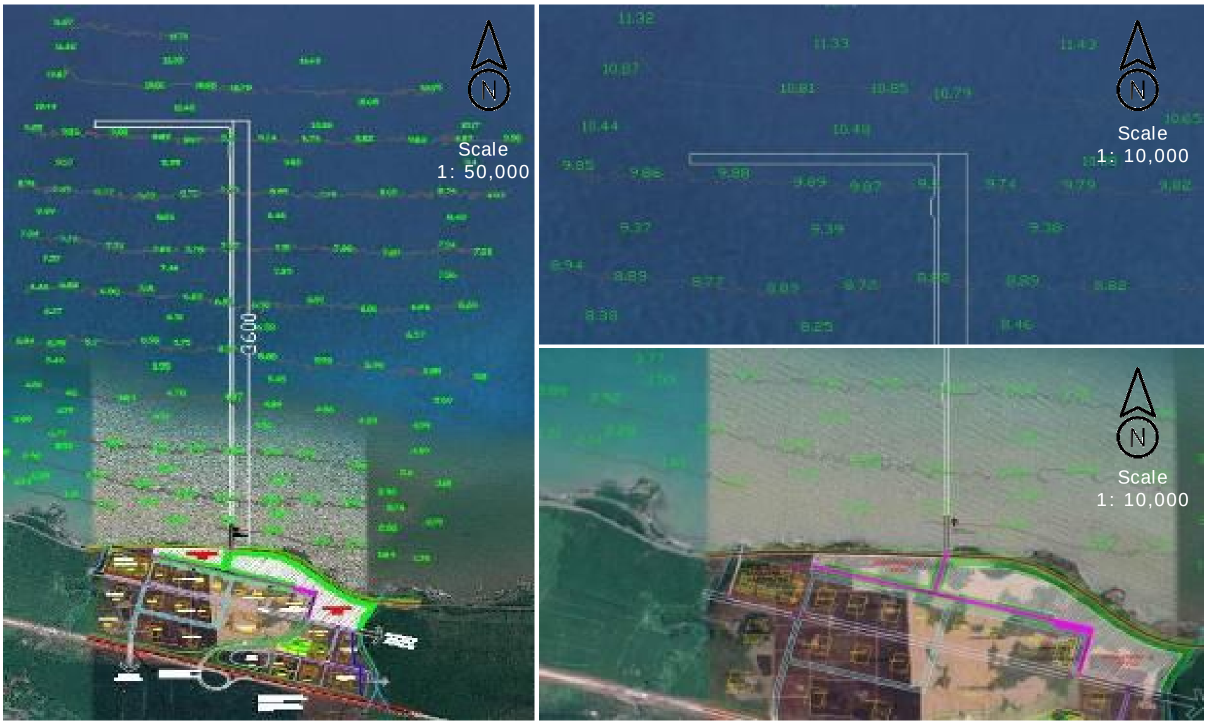

Figure 3. Bathymetric survey results at port locations.

Existing hydrographic data and analysis. This analysis consists of two parts consisting of tidal observation analysis and tidal harmonic analysis.

Tidal observation analysis. Tidal measurements at the survey location were carried out on August 25 - September 9, 2020. By using an automatic tidal height recorder (tide gauge) placed in the survey area. The tide gauge records variations in sea level every 15 minutes.

From the Figure 4, it can be seen that the two graphs are similar to each other, especially the time of arrival of high and low tides and also have a small root mean square error (RMSE) of 0.04 m (4.7%).

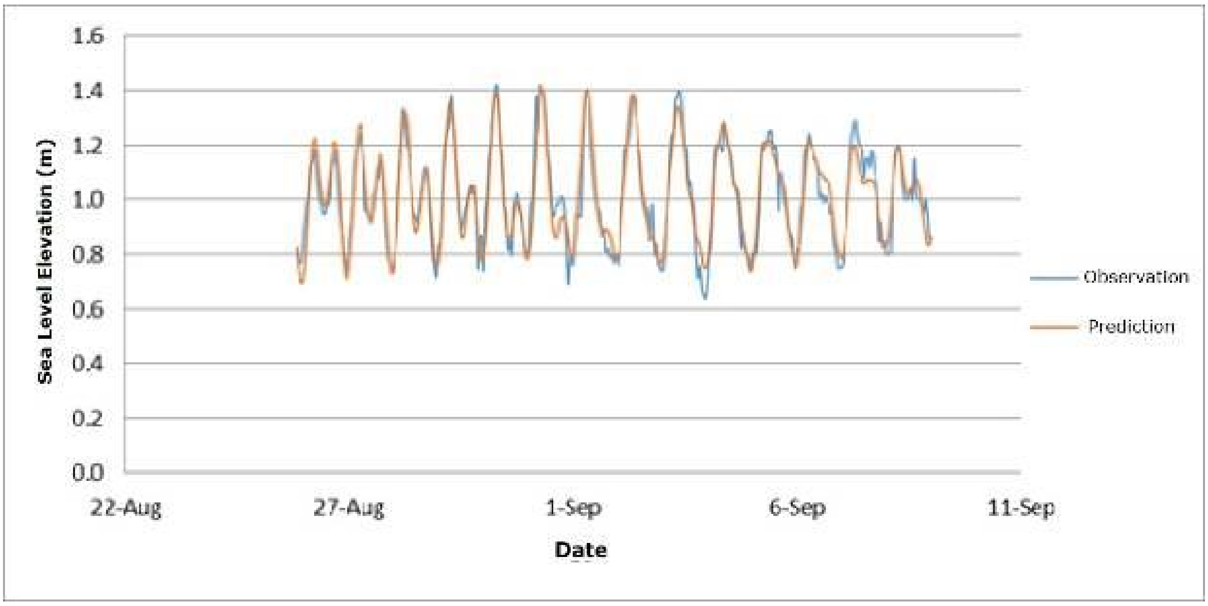

Figure 4. Tidal chart measurement and prediction in the waters of the Plabuan Station, Batang Regency.

Tidal harmonic analysis. The tides are generated by the attraction of the moon, sun and other celestial bodies, which are called astronomical factors. Throughout the propagation of tidal waves are influenced by the topography of the seabed, beach morphology and meteorological conditions (Triatmodjo 1999). The tidal component produced by astronomical factors is a harmonic wave (periodic), while the meteorological effect is not periodic, and often only produces a momentary effect.

To test the accuracy of the results of the tidal harmonic analysis, a verification process is carried out by predicting the tidal height at the same time as data collection. From the verification results, it was found that the harmonic analysis carried out was quite good, as shown in the Table 1. To calculate the significant figures of the tides, the results of the harmonic analysis are used as the basis for forecasting the tides for 6789 days (18.6 years). From the results of the tidal analysis, the important tidal figures are obtained on the Table 1.

Table 1

Tides important elevation value

Parameter	*Level against LWS (m)*	*Number of occurrence in 18.6 years*
Highest astronomical tide (HAT)	1.06	1
Mean higher water spring (MHWS)	0.95	493
Mean lower high water spring (MLHW)	0.76	8101
Mean sea level (MSL)	0.55	175320
Mean higher low water spring (MHLWS)	0.33	8181
Mean lower water spring (MLWS)	0.16	493
Lowest astronomical tide (LAT)	0.00	1
	Tidal range 1.06 m	

Ocean current observation data and analysis. Data collection activities were carried out at 2 ADCP locations on 9-11 September 2020, with data samples every 10 minutes, (see Figure 5 and Table 2) and 4 current meter locations for 24 hours at each location. Measurements at each station and each measurement event were carried out at three depths (d), namely at every 0.2 depths, 0.6 depths and 0.8 depths (see Figure 6 and Table 3). Measurements were made using the Current Meter OTT Hydrological Services Germany serial number 055-BI 98-28.

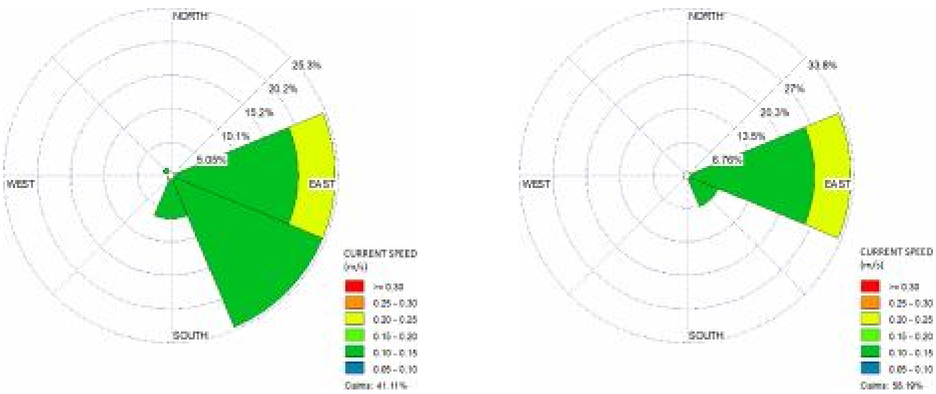

Figure 5. Documentation of Current Rose ADCP ST01 (left) and ADCP ST02 (right).

Table 2

Current velocity profile against depth (ADCP)

Sea level depth (m)	*Cell*	*ADCP ST01*			*ADCP ST02*		
		Current speed (m s^{-1})			*Current speed (m s^{-1})*		
		Average	*Max*	*Min*	*Average*	*Max*	*Min*
1	10	0.37	0.67	0.04	0.37	0.71	0.02
2	9	0.08	0.19	0.01	0.08	0.30	0.00
3	8	0.08	0.21	0.01	0.07	0.20	0.00
4	7	0.08	0.20	0.01	0.07	0.20	0.00
5	6	0.07	0.18	0.01	0.07	0.19	0.00
6	5	0.08	0.21	0.00	0.07	0.22	0.00
7	4	0.07	0.18	0.01	0.08	0.22	0.00
8	3	0.07	0.22	0.01	0.08	0.22	0.00
9	2	0.06	0.17	0.00	0.07	0.18	0.00
10	1	0.07	0.19	0.01	0.06	0.16	0.00

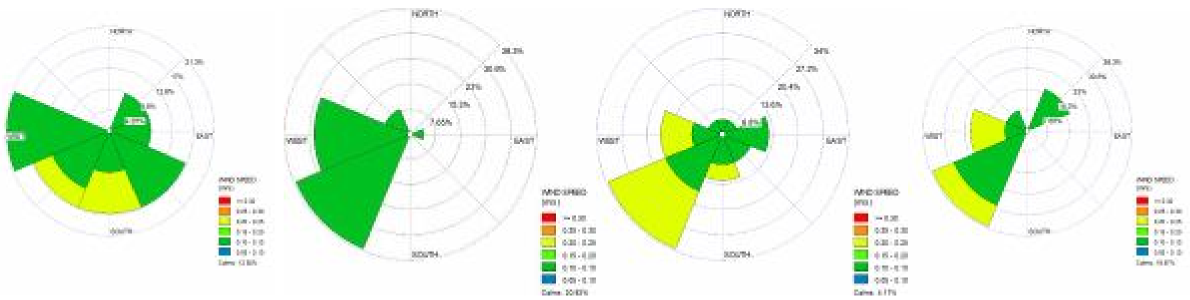

Figure 6. Current Rose CM1, CM2, CM3, and CM4.

Table 3

Current velocity profile against depth (current meter)

Location	*Depth*	*Current speed (m s^{-1})*		
		Average	*Max*	*Min*
CM1	0.2 d	0.16	0.24	0.06
	0.6 d	0.12	0.21	0.05
	0.8 d	0.10	0.16	0.04
CM2	0.2 d	0.10	0.20	0.05
	0.6 d	0.07	0.12	0.04
	0.8 d	0.06	0.12	0.04
CM3	0.2 d	0.12	0.20	0.05
	0.6 d	0.12	0.20	0.06
	0.8 d	0.12	0.21	0.04
CM4	0.2 d	0.13	0.22	0.05
	0.6 d	0.11	0.21	0.05
	0.8 d	0.11	0.20	0.05

Wind and wave modeling. The wind causes ocean waves, therefore wind data can be used to estimate the height and direction of waves at the study site. Considering that wave data from field measurements are not available, and even if there is only a brief note, the data does not reflect the overall wave conditions, then for the planning of wave heights at the port location an approach will be used through the results of wave forecasts based on wind data. Wind data is needed as input data in wave forecasting so that the design wave height is obtained. The wind data taken is the wind in the deep sea with a distance of about 35 km from the port location.

The wind data used is sourced from The European Centre for Medium-Range Weather Forecast (ECMWF), because the nearest Badan Meteorologi, Klimatologi, dan Geofisika (BMKG) wind data is in Semarang City, which is 47 km away and only daily average data can be obtained, so the data cannot be analyzed for return periods or wave hidcasting.

Surface wind conditions (secondary wind data). Wind conditions around the study site are represented by wind data taken at coordinates 6°35'46.95" South Latitude and 109°57'2.73" East Longitude. The wind conditions are presented through wind roses to get an overview of the wind distribution at the study site. The results of the analysis of wind conditions are presented in Table 4, Figure 7 and Figure 8.

Based on the distribution in Figure 7 and Figure 8, it can be seen that during the recorded data, the dominant wind in the waters around the Supporting Port of KIT Batang blows towards the east and west. The winds that form in one year are seen to be influenced by two wind seasons. The west monsoon is dominated by winds blowing from the west and northwest for four months, from December to March. Meanwhile, the east monsoon is dominated by the wind that blows from the east for 6 months, from May to October. The transition season occurs in April and November.

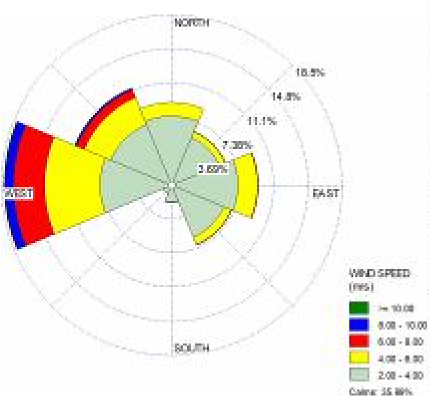

Directions	2.0 - 4.0	4.0 - 6.0	6.0 - 8.0	8.0 - 10.0	>=10.0	Total (%)
N	7.50	1.42	0.00	0.00	0.00	8.93
NE	5.62	0.67	0.04	0.00	0.00	6.33
E	7.20	2.10	0.07	0.00	0.00	9.38
SE	6.15	0.86	0.06	0.00	0.00	7.06
S	1.88	0.07	0.00	0.00	0.00	1.95
SW	1.02	0.02	0.00	0.00	0.00	1.04
W	7.76	5.97	3.36	0.92	0.07	18.09
NW	7.13	3.09	0.91	0.19	0.02	11.34
Sub-Total	44.27	14.21	4.44	1.11	0.09	64.11
Calms						35.89
Total						100.00

Figure 7. Wind distribution around waters (ECMWF).

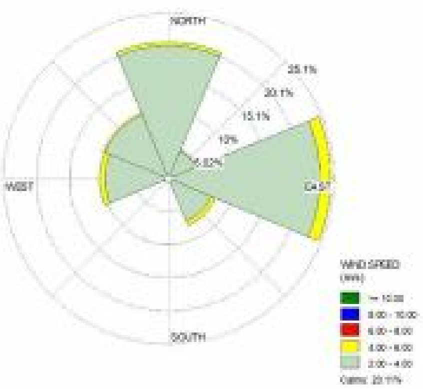

Directions	2.0 - 4.0	4.0 - 6.0	6.0 - 8.0	8.0 - 10.0	>=10.0	Total (%)
N	20.11	0.54	0.00	0.00	0.00	20.65
NE	4.48	0.14	0.00	0.00	0.00	4.62
E	22.96	1.63	0.00	0.00	0.00	24.59
SE	7.07	0.68	0.00	0.00	0.00	7.74
S	0.41	0.00	0.00	0.00	0.00	0.41
SW	0.68	0.00	0.00	0.00	0.00	0.68
W	9.65	0.82	0.00	0.00	0.00	10.46
NW	10.46	0.27	0.00	0.00	0.00	10.73
Sub-Total	75.82	4.08	0.00	0.00	0.00	79.89
Calms						20.11
Total						100.00

Figure 8. Wind distribution around waters (BMKG).

Table 4

Maximum wind speed in each direction (ECMWF)

Year	*Maximum wind speed* ($m\ s^{-1}$)							
	N	*NE*	*E*	*SE*	*S*	*SW*	*W*	*NW*
2010	5.1	5.6	6.9	6.3	3.3	4.9	9.8	10.1
2011	5.8	6.1	5.6	4.9	4.0	4.1	11.1	9.9
2012	5.2	4.9	5.9	5.8	4.2	3.9	11.6	11.6
2013	6.0	6.1	7.8	8.0	3.6	5.4	10.4	11.2
2014	5.5	6.1	7.1	7.0	4.1	4.2	10.7	10.4
2015	5.7	6.5	7.1	7.3	3.8	4.7	9.5	9.4
2016	5.0	5.4	6.2	6.1	3.6	3.9	9.2	8.6
2017	5.6	7.5	7.4	6.9	4.1	3.9	10.2	10.5
2018	5.7	5.3	5.8	6.4	5.0	4.3	9.4	10.0
2019	5.7	6.5	6.3	5.7	4.4	4.2	10.0	10.0

Metaocean numerical modeling of Batang Integrated Industrial Estate port. The numerical model analysis in this study is in the form of modeling ocean currents, waves and sedimentation. The intended modeling area can be seen in the Figure 9. This model aims to determine the pattern of currents, waves and areas of abrasion and deposition areas at the study site. The data used to build the model are surveys and secondary data.

Figure 9. Model area.

Existing wave model. The input data for the modeling of the global wave ECMWF Spectral Waves (SW) module are the wave data and the hindcasting (Hs) wave data (Figure 10 and Figure 11). This model was run for 10 years to get an idea of the wave height.

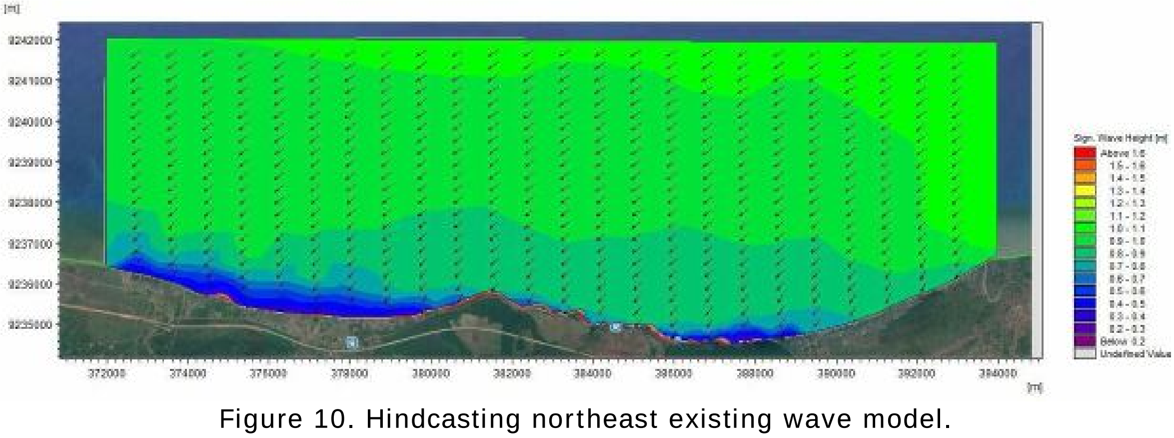

Figure 10. Hindcasting northeast existing wave model.

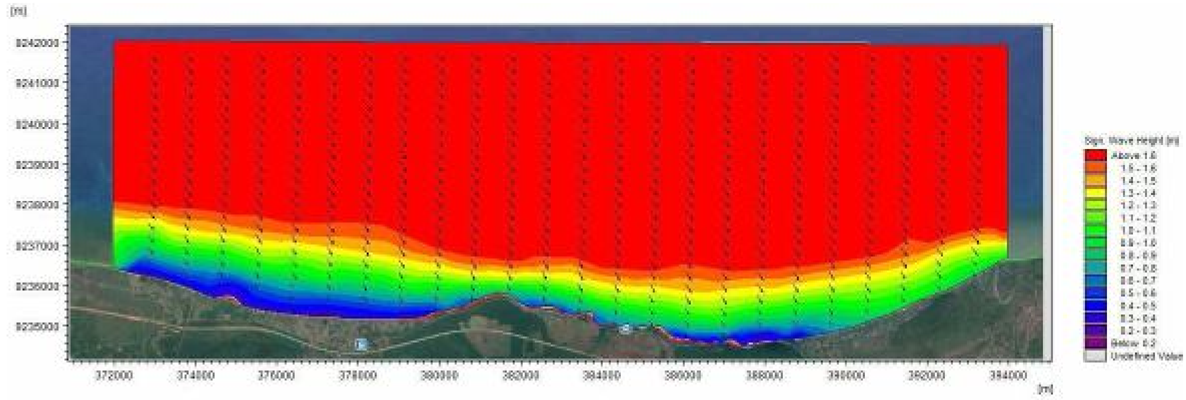

Figure 11. Hindcasting northwest existing wave model.

Wave model (ECMWF). Since the location of the proposed wharf is an open sea, the wave model with ECMWF input waves is more suitable because the ECMWF wave data is a combination of wind waves and swells which predominantly occur in open water. The wave conditions in each alternative are relatively the same because they are both open areas and have equally sloping depth contours (Figure 12).

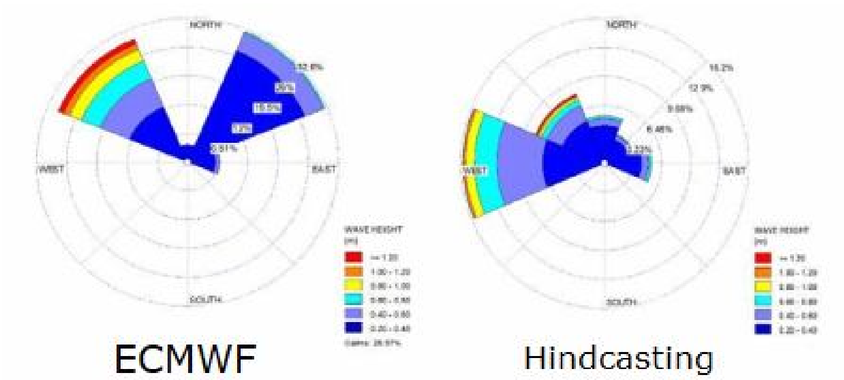

Figure 12. Wave model distribution (ECMWF) and port plan location hindcasting.

Current and sediment model (existing). At high tide (Figure 13), the dominant current flows towards the west, while at low tide (Figure 14) the dominant current flows towards the east. The flow rate for all alternatives is the same on a relatively small wharf plan.

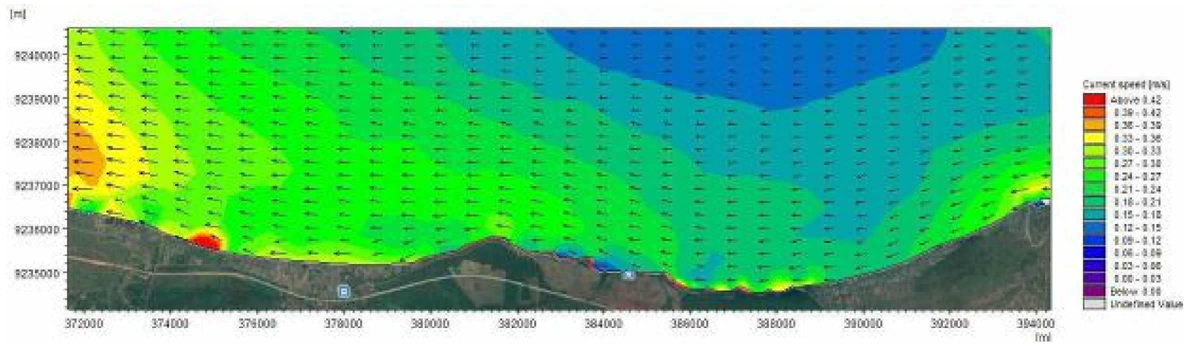

Figure 13. Current pattern high tide in spring tide conditions.

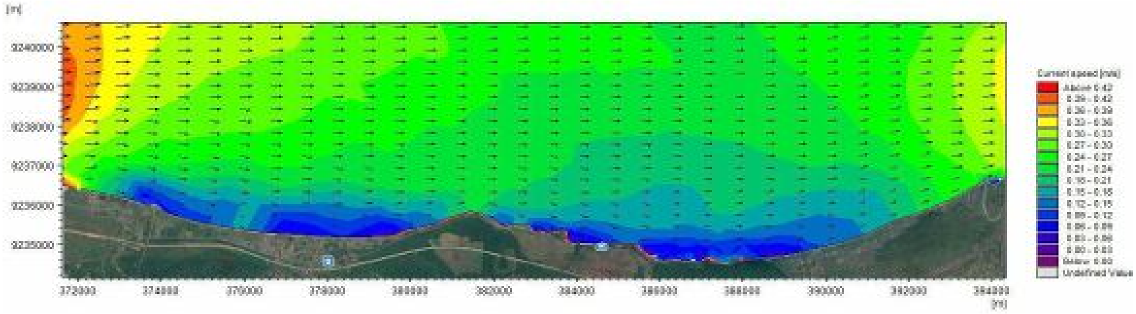

Figure 14. Current pattern at low tide in spring tide conditions.

The concentration of suspended sediment is spread between 0.002 and 0.02 kg m^{-3} (2-20 mg L^{-1}), the concentration of suspended sediment is very small in this estuary area, this is because sediment collection is carried out in the dry season. The highest concentration occurs in the estuary area, while the lowest is in the offshore area (Figure 15 and Figure 16). The distribution of sediment originating from the river does not reach the pier design area.

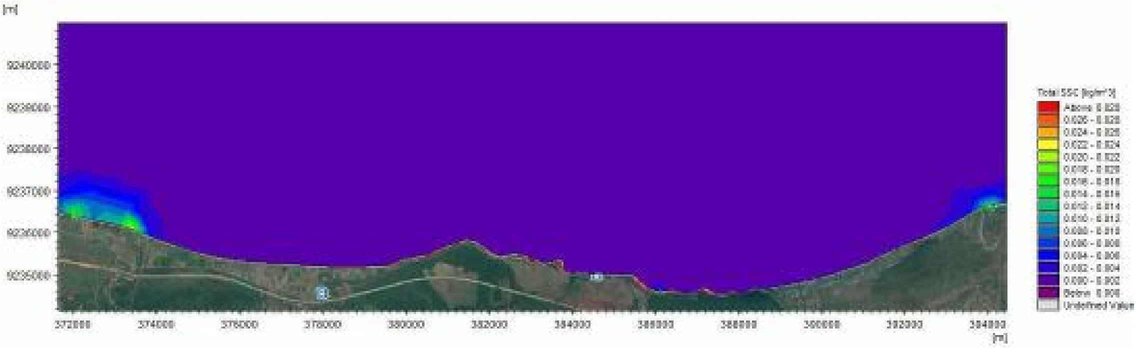

Figure 15. Simulation results of floating sediment concentration at high tide.

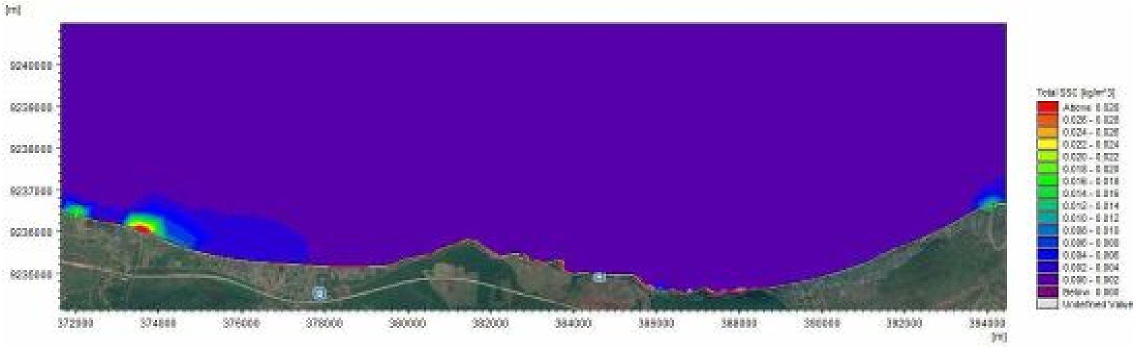

Figure 16. Simulation results of floating sediment concentration at low tide.

The processed results at the observation point show a trend of increasing the thickness of the sediment layer over a period of 25 years. Based on the analysis of changes in the bottom layer of the waters, the potential sedimentation rate at the observation point is 0.0185 m for 25 years (Figure 17).

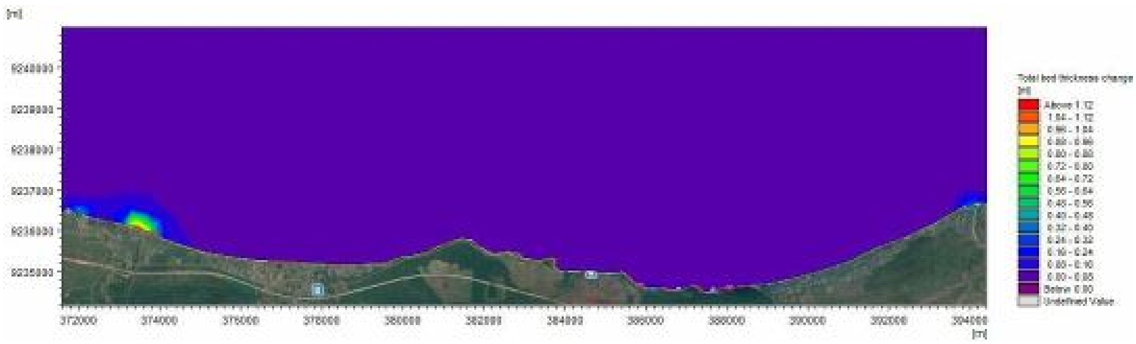

Figure 17. Pattern of changes in the seabed for 25 years.

Discussion

Trestle length to reach planned depth. As stated in the previous section, to achieve the desired pool depth of 10 mlws, the pier to be built will use a trestle with a distance of 3.6 km from the shoreline. Based on the desk study conducted by considering currents, waves, and winds as discussed above, the pier which is 3.6 km (Figure 18) from the shoreline must be protected by a breakwater. The type of breakwater that is recommended in this study is offshore breakwater, this type of breakwater is intended for optimization of fishing areas that can be maintained compared to the type of shore-connected breakwater. The next section will discuss the comparison of the area lost when using offshore breakwater and shore-connected breakwater.

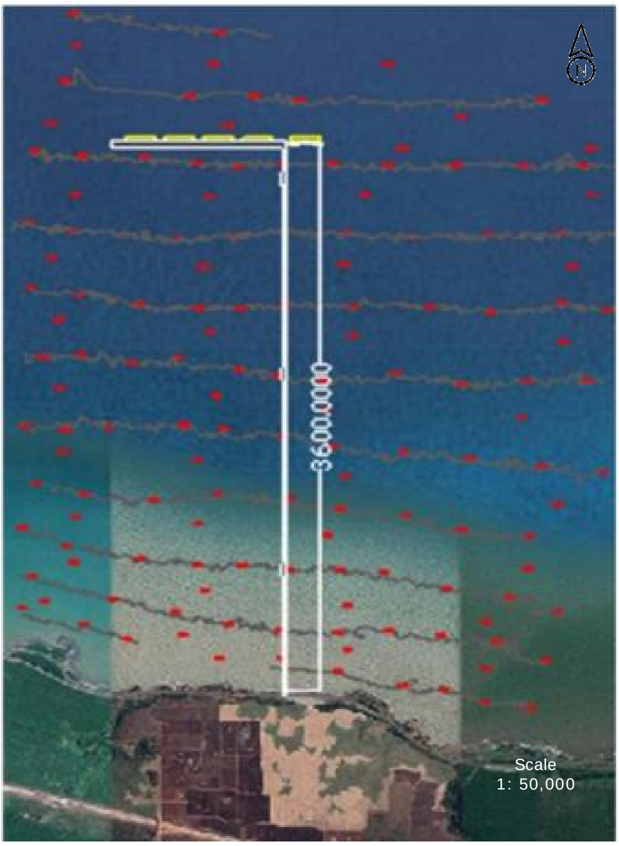

Figure 18. Trestle length at harbor location.

Potential lost fishing area with shore-connected breakwater. The analysis then continues what if the type of breakwater boundary used is shore-connected like the surrounding ports. Searching through GIS tools proves that under these conditions the area that will belong to the port or in other words the area of fishing that will be lost reaches 669.59 hectares (Figure 19).

Considering that the construction of the port is part of the national economic recovery, especially to respond to the Covid-19 pandemic, public planning policies must take advantage of existing fishery activities. Such stakeholder engagement will increase project sustainability and will reduce coastal resource conflicts (Ditty & Rezende 2014). In this study, modeling was carried out for the shape of the offshore breakwater in order to take advantage of existing fishery activities. It is possible that the utilization of fishery activities will be carried out if there are no obstacles in the technical aspects of the port, especially the pier, such as aspects of waves, currents, and sedimentation.

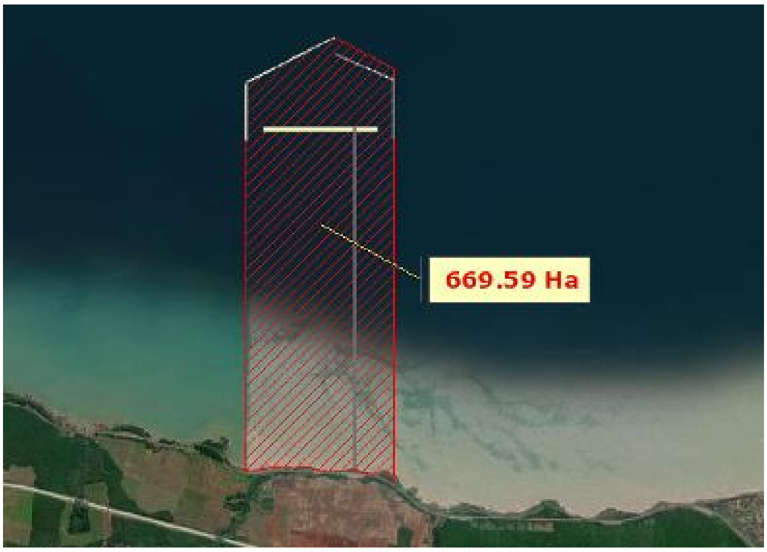

Figure 19. Lost fshing area with shore-connected breakwater.

Offshore breakwater shape*.* The analysis then proceeds to modeling the breakwater when the boundary does not reach the shoreline, but optimizes its shape according to its function in regulating the entry and exit of container ships. The recommended breakwater shape can be seen in Figure 20. With the shape of a breakwater like this which of course does not reach the shoreline, the area that can still be used as a fishing area is 548.41 hectares (81.90% of total area if using connected-shore breakwater).

Figure 20. Offshore breakwater shape (left); lost fishing area with offshore breakwater (right).

Port technical analysis with offshore breakwater*.* The results of the modeling show that there is no disturbance to port activities, both from a technical point of view and the growth of sediment, which in aggregate is considered the cause of port operational failure. More about this can be seen in the following analysis.

Wave model with offshore breakwater. The post-construction model is a model that was built with a offshore breakwater scenario which aims to make the wharf operation time run for one full year, from the simulation results with breakwaters on all alternative wave heights of Hs less than 0.4 m (Figure 21 and Figure 22), this means that with an off shore breakwater scenario operating time can be up to 1 full year.

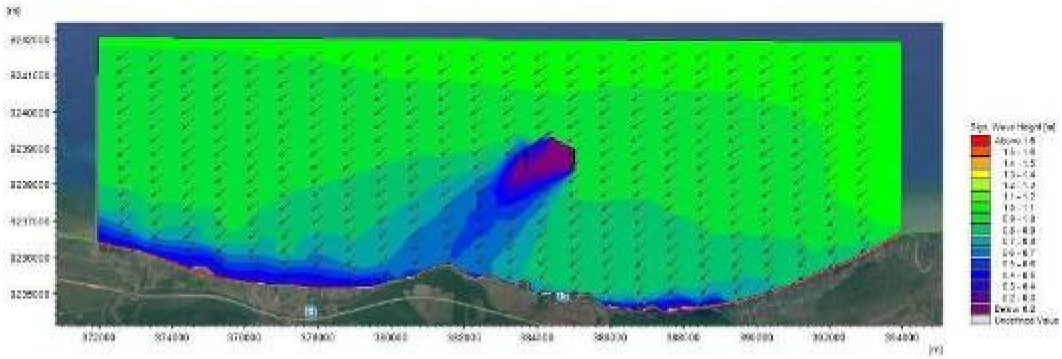

Figure 21. Hs wave model (with offshore breakwater) northeast.

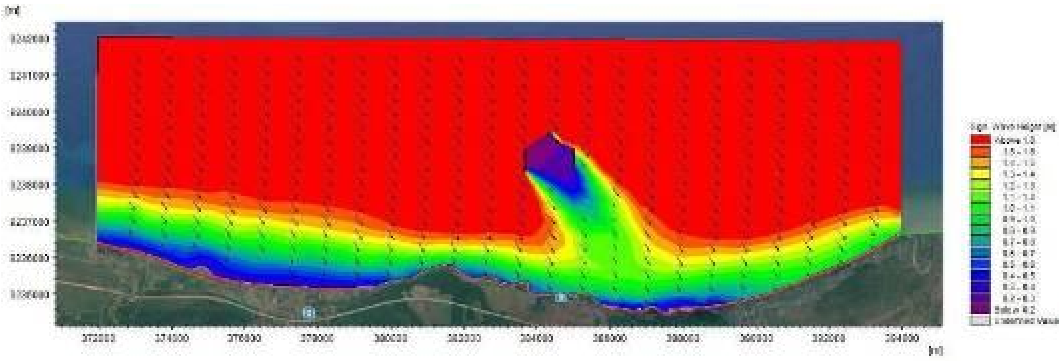

Figure 22. Hs wave model (with offshore breakwater) northwest.

Current flow and sedimentation model with offshore breakwater. The results of the current and sedimentation modeling with the offshore breakwater scenario can be seen in the Figure 23 and Figure 24. Current simulation results with offshore breakwaters in all alternatives are relatively the same, having a maximum current speed of 0.1 m s^{-1}.

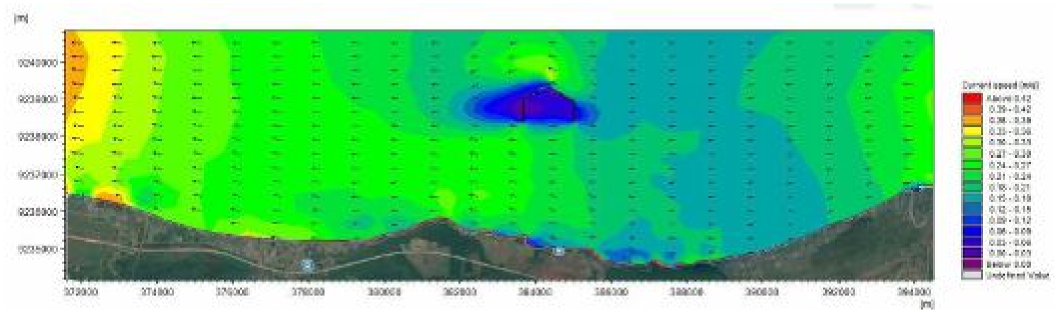

Figure 23. Current pattern at high tide with offshore breakwater.

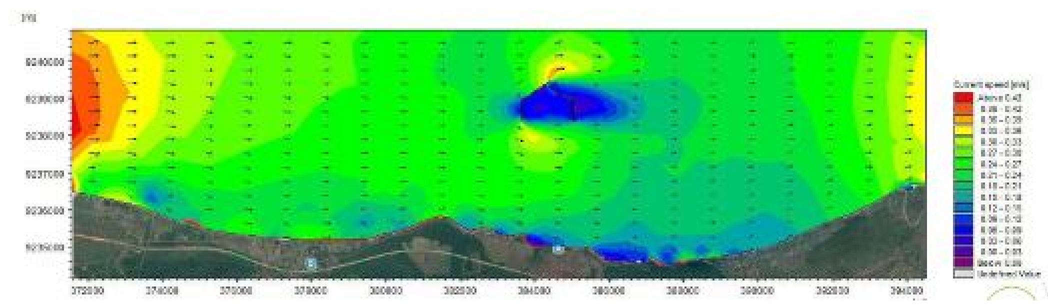

Figure 24. Current pattern at low tide with offshore breakwater.

The results of the post-port construction sedimentation model with a offshore breakwater, where the sedimentation in the area shows a pattern of changes in the bottom of the waters for 25 years (Figure 25), experiencing an increase in the bottom of the water by 0.0172 m, this condition is relatively the same as the existing condition.

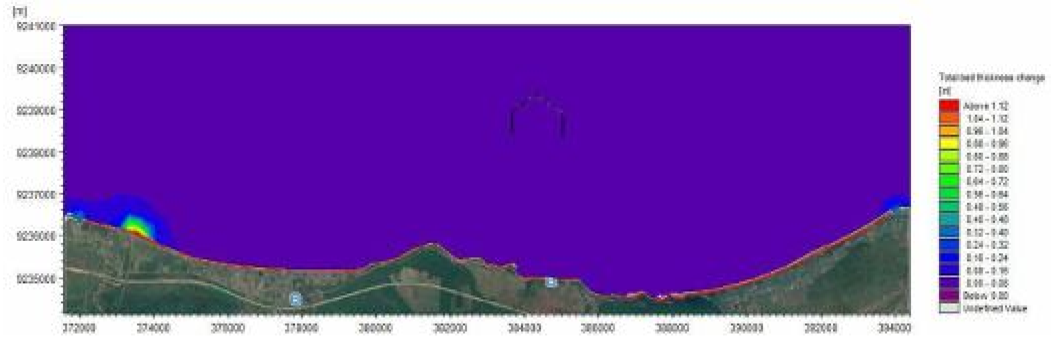

Figure 25. Pattern of changes in the seabed for 25 years (with offshore breakwater).

Comparison of existing models with offshore breakwater models. The modeling results show that the average current velocity of the entire depth around the pier when the existing condition reaches 0.66 m s^{-1} and during the post-construction condition is 0.1 m s^{-1}. The results of the sedimentation of the existing and post-construction models around the pier location are not very different because the distribution of sediment from the river mouth does not reach the design area of the pier. The maximum existing Hs wave height reaches 1.91 m with a port operating time of 81 days for one year. The maximum Hs wave height after the breakwater construction reaches 0.35 m with a port operating time of one full year.

Conclusions. The interaction between the two sectors in the study area, namely the container port sector and the capture fisheries sector, can lead to increased social tensions and reduced community cohesion. Of course, this needs to be avoided in order to create and maintain sustainable coastal communities in accordance with what is stated by the Marine Management Organization.

From the results of the analysis that has been carried out, using an offshore breakwater design, the fishing area that can still be used by fishermen is 548.41 hectares (81.91% of 669.59 hectares). In other words, the area lost due to port activities is 121.18 hectares (18.09%), from the previous total lost area of 669.59 hectares when using the shore-connected breakwater design. The important point is that there is no technical disruption to port activities when the breakwater design is implemented as recommended above.

Thus, the port development which is part of the National Economic Recovery strategy can minimize the environmental and economic impact of the fishing community. In the end, port development which is expected to be able to increase economic value is not only seen in terms of macroeconomic value, but rather to create shared value on a microeconomic scale, namely port development that is synergistic with the utilization of existing fishery activities. In other words, the development of existing port infrastructure does not eliminate the economic activities of the people at the construction site.

Conflict of interest. The authors declare that there is no conflict of interest.

References

Ariansyach I., 2017 Fisheries country profile: Indonesia. SEAFDEC Southeast Asian Fisheries Development, Bangkok. Available at: www.seafdec.org/fisheries-country-profile-indonesia/. Accessed: October, 2020.

Bonar G. P., 2014 Evaluasi dan re-design breakwater untuk pelabuhan penyeberangan (Feri) waikelo, kaabupaten sumba barat, Nusa Tenggara timur. Undergraduate thesis, Institut Teknologi Sepuluh Nopember, 164 pp. [in Indonesian]

Badan Pusat Statistik (BPS), 2020 Kabupaten Batang Dalam Angka 2020. Available at: https://batangkab.bps.go.id/publication/2020. Accessed: 10 August 2020. [in Indonesian]

Coastal Engineering Research Center (CERC), 1984 Shore protection manual. Volume I. US Army Corps of Engineers, Washington DC, 597 pp.

Ditty J. M., Rezende C. E., 2014 Unjust and unsustainable: a case study of the Açu port industrial complex. Marine Policy 45:82-88.
Dunford M., Yeung G., 2020 Development, regional, port-industrial complexes. In: International encyclopedia of human geography. 2nd edition. Kobayashi A. (ed), Elsevier, pp. 271-280.
FAO, 2014 Fishing and aquaculture country profiles: the Republic of Indonesia. Food and Agriculture Organization of the United Nations, Rome. Available at: http://www.fao.org/fishery/facp/IDN/en. Accessed: September, 2020.
Farliana N., Setiaji K., Melati I. S., Hardianto H., 2020 The impact of Kendal Industrial Park (Indonesia-Singapore Cooperation) in economic perspective. International Journal of Scientific and Technology Research 9(3):4407-4414.
Park Y., Dossani R., 2020 Port infrastructure and supply chain integration under the belt and road initiative: role of Colombo Port in the apparel industry in South Asia. Transportation Research Procedia 48:307-326.
Pelindo 3, 2020 Studi Kelayakan (FS) Penyediaan Pelabuhan Pendukung Kawasan Industri Terpadu Batang. [in Indonesian]
Peraturan Pemerintah Republik Indonesia Nomor 23 Tahun 2020 tentang Pelaksanaan Program Pemulihan Ekonomi Nasional dalam Rangka Mendukung Kebijakan Keuangan Negara untuk Penanganan Pandemi Corona Virus Disease 2019 (COVID-19) dan/atau Menghadapi Ancaman yang Membahayakan Perekonomian Nasional dan/atau Stabilitas Sistem Keuangan serta Penyelamatan Ekonomi Nasional, diterbitkan 11 Mei 2020. [in Indonesian]
Peraturan Presiden (PERPRES) Nomor 79 Tahun 2019 tentang Peraturan Presiden (PERPRES) tentang Percepatan Pembangunan Ekonomi Kawasan Kendal - Semarang - Salatiga - Demak - Grobongan, Kawasan Purworejo - Wonosobo - Magelang - Temanggung, dan Kawasan Brebes - Tegal – Pemalang, diterbitkan 25 November 2019. [in Indonesian]
Peraturan Presiden (PERPRES) Nomor 109 Tahun 2020 tentang Perubahan Ketiga atas Peraturan Presiden Nomor 3 Tahun 2016 tentang Percepatan Pelaksanaan Proyek Strategis Nasional, diterbitkan 20 November 2020. [in Indonesian]
Purwanto, 2003 Status and management of the Java Sea fisheries. WorldFish Center and Asian Development Bank, pp. 793-832.
Triatmodjo B., 1999 Teknik pantai. Beta Offset. Yogyakarta, 69 pp. [in Indonesian]
Wan C., Tao J., Wu J., Zhang D., 2020 [An analysis of influences of the Covid-19 on the spatial structure of the China's global shipping network]. Journal of Transport Information and Safety 38(2):129-135. [in Chinese]
Warren C., Steenbergen D. J., 2021 Fisheries decline, local livelihoods and conflicted governance: an Indonesian case. Ocean and Coastal Management 202:105498.

Received: 16 January 2022. Accepted: 12 February 2022. Published online: 11 March 2022.
Authors:
Okto R. Manullang, Department of Urban and Regional Planning, Faculty of Engineering, Diponegoro University, Prof. Soedarto street, SH, Tembalang, Semarang, Central Java, Indonesia 50275, e-mail: oktomanullang@lecturer.undip.ac.id
Andi Prasetiawan, Merchant Marine Polytechnic Semarang, Singosari Raya street, No. 2A, Wonodri, Semarang, Central Java, Indonesia 50242, e-mail: andiprasetiawan@pip-semarang.ac.id
Paldibo A. Sitorus, Department of Urban and Regional Planning, Faculty of Engineering, Diponegoro University, Prof. Soedarto street, SH, Tembalang, Semarang, Central Java, Indonesia 50275, e-mail: alfriramson@gmail.com

How to cite this article:
Manullang O. R., Prasetiawan A., Sitorus P. A., 2022 Analysis of port breakwater boundaries in optimizing fishing areas in Batang integrated industrial area. AACL Bioflux 15(2):593-607.